Scaled Quantum Chemical Studies on the Vibrational Spectra of 2,5-Dichloroaniline

M.K.Subramanian* and P.Salomi

Post Graduate and Research Department of Physics, Thiruvalluvar Government Arts College, Rasipuram, India.

ARTICLE INFO

ABSTRACT

In this work, the experimental and theoretical study on vibrational spectra of 2,5-Dichloroaniline (25DCA) were studied. The molecular structure, fundamental vibrational frequencies and intensity of the vibrational bands are interpreted with the aid of structure optimizations and normal coordinate force field calculations based on density functional theory (DFT) using B3LYP method with 6-311+G** basis set combination. Complete vibrational assignment and analysis of the fundamental modes of the compound were carried out using the observed FT-IR and FT Raman data. Simulated FTIR and FT Raman spectra for 25DCA showed good agreement with the observed spectra. Mulliken analysis of atomic charges is also calculated. The calculated HOMO–LUMO energies shows that charge transfer occur within the molecule. The dipole moment (μ) and First-order hyperpolarizability (β_0) of the molecule have been reported. Electronic excitation energies, oscillator strength and nature of the respective excited states were calculated by the closed-shell singlet calculation method for the molecule.

Introduction

Aniline, phenylamine or aminobenzene is an organic compound. It is the simplest and one of the most important aromatic amines, being used as a precursor to more complex chemicals. Its main application is in the manufacture of polyurethane. Like most volatile amines, it possesses the unpleasant odour of rotten fish and also has a burning aromatic taste; it is a highly-acrid poison. It ignites readily, burning with a smoky flame.

Quantum chemical computational methods have proved to be an essential tool for interpreting and predicting the vibrational spectra. A significant advance in this area was made by scaled quantum mechanical (SQM) force field method. In scaled quantum mechanical (SQM) approach, the systematic errors of the computed harmonic force field are corrected by a few scale factors which are found to be well transferable between chemically related molecules and were recommended for general use. Recent spectroscopic studies on these materials have been motivated because the vibrational spectra are very useful for the understanding of specific biological process and in the analysis of relatively complex systems.

In this work, we apply the density functional theory to study the vibrational spectra and structure of 2,5-dichloroaniline (25DCA). The calculated Infrared and Raman spectra of the title compounds were also stimulated utilizing the scaled force fields and the computed dipole derivatives for IR intensities and polarisability derivatives for Raman intensities.

Experimental Details

The compound 25DCA was purchased from the Sigma–Aldrich Chemical Company (USA) with a stated purity of greater than 98% and it was used as such without further purification. The FT-Raman spectra of 25DCA was recorded using 1064 nm line of Nd:YAG laser as excitation wavelength in the region 4000–100 cm^{-1} on a Brucker model IFS 66 V spectrophotometer equipped with FRA 106 FT-Raman module accessory. The room temperature FT-IR spectrum of this compound was recorded in the region 4000-400 cm^{-1} on IFS 66V spectrophotometer using KBr pellet technique.

Computational Details

All calculations were performed using GAUSSIAN 09W program package [1] and the vibrational modes were assigned by means of visual inspection using GAUSSVIEW program and also from the results of normal co-ordinate calculations. The geometry optimization and energy calculations of conformers of 25DCA were carried out using DFT (B3LYP) methods [2,3] with 6-31G* and 6-311+G** basis sets, respectively. The Cartesian representation of the theoretical force constants have been computed at optimized geometry by assuming C$_s$ point group symmetry, scaling of the force fields were performed by the scaled quantum mechanical procedure [4].

The symmetry of the molecule was also helpful in making vibrational assignments. The symmetries of the vibrational modes were determined by using the standard procedure [5,6] of decomposing the traces of the symmetry operation into the irreducible representations. The symmetry analysis for the vibrational mode of 25DCA is presented in some details in order to describe the basis for the assignments. By combining the results of the GAUSSVIEW program [7] with symmetry considerations, vibrational frequency assignments were made with a high degree of confidence.

The prediction of Raman intensities was carried out by following the procedure outlined below. The Raman activities (*Si*) calculated by the GAUSSIAN 09W program and adjusted during scaling procedure with MOLVIB were converted to relative Raman intensities (*Ii*) using the following relationship derived from the basic theory of Raman scattering [8-9].

$$I_i = \frac{f(v_o - v_i)^4 S_i}{v_i[1 - \exp(-hcv_i / KT)]} \quad \text{--------------(1)}$$

Where v_0 is the exciting frequency (in cm^{-1}), v_i is the vibrational wavenumber of the ith normal mode; h, c and k are fundamental

Tele:
E-mail addresses: profdrmks@gmail.com

constants, and f is a suitably chosen common normalization factor for all peak intensities.

Essentials of nonlinear optics related to β

The nonlinear response of an isolated molecule in an electric field $E_i(\omega)$ can be represented as a Taylor expansion of the total dipole moment μ_t induced by the field:

$$\mu_t = \mu_0 + \alpha_{ij}E_i + \beta_{ijk}E_iE_j + \ldots\ldots$$

Where α is linear polarizability, μ_0 the permanent dipole moment and β_{ijk} are the first-order hyperpolarizability tensor components. The components of first-order hyperpolarizability can be determined using the relation

$$\beta_i = \beta_{iii} + \frac{1}{3}\sum_{i\neq j}(\beta_{ijj} + \beta_{jij} + \beta_{jji})$$

Using the x, y and z components the magnitude of the total static dipole moment (μ), isotropic polarizability (α_0), first-order hyperpolarizability (β_{total}) tensor, can be calculated by the following equations:

$$\mu_1^0 = (\mu_x^2 + \mu_y^2 + \mu_z^2)^{1/2}$$

$$\beta_{tot} = (\beta_x^2 + \beta_y^2 + \beta_z^2)^{1/2}$$

The complete equation for calculating the first-order hyperpolarizability from GAUSSIAN 09W output is given as follows:

$$\beta_{tot} = [(\beta_{xxx} + \beta_{xyy} + \beta_{xzz})^2 + (\beta_{yyy} + \beta_{yzz} + \beta_{yxx})^2 + (\beta_{zzz} + \beta_{zxx} + \beta_{zyy})^2]$$

The β components of GAUSSIAN 09W output are reported in atomic units, the calculated values have to be converted into electrostatic units (1 a.u= 8.3693 x10^{-33} esu).

Molecular geometries were fully optimized by Berny's optimization algorithm using redundant internal coordinates. All optimized structures were confirmed to be minimum energy conformations. An optimization is complete when it has converged. i.e., when it has reached a minimum on the potential energy surface, thereby predicting the equilibrium structures of the molecules. This criterion is very important in geometry optimization. The inclusion of d polarization and double zeta function in the split valence basis set is expected to produce a marked improvement in the calculated geometry. At the optimized structure, no imaginary frequency modes were obtained proving that a true minimum on the potential energy surface was found. The electric dipole moment and dispersion free first-order hyperpolarizibility were calculated using finite field method. The finite field method offers a straight forward approach to the calculation of hyperpolarizabilities. All the calculations were carried out at the DFT level using the three-parameter hybrid density functional B3LYP and a 6-311+G** basis set.

Results and discussion

Structural description

The optimized molecular structure with the numbering of atoms of the title compound is shown in Fig 1. In order to find the most optimized geometry, the energy calculations were carried out for 25DCA using B3LYP/6-311+G** method. The total energies obtained for were listed in Table 1.

Table 1. Total energies of 25DCA, calculated at DFT B3LYP/6-31G* and B3LYP/6-311+G level**

Method	Energies (Hartrees)
6-31G*	-1206.68852401
6-311+G**	-1206.79536602

It is clear from the Table 1 the structure optimizations have shown that the B3LYP/6-311+G** have produced the global minimum energy. The most optimized structural parameters were also calculated and they were depicted in Table 2.

Normal coordinate analysis were carried out to provide a complete assignment of the fundamental vibrational frequencies for the molecule for this purpose the full set of standard internal coordinates (containing-redundancies) were defined as given Table 3. From these a non-redundant set local symmetry coordinates were constructed by suitable linear combinations of internal coordinates following the recommendations of Fogarasi and Pulay [4] and they are presented in Table 4. The theoretically calculated force field were transformed to this later set of vibrational coordinates and used in all subsequent calculations.

Potential energy distribution

To check whether the chosen set of symmetric coordinates contribute maximum to the potential energy associated with the molecule, the PED has been carried out. The vibrational problem was set-up in terms of internal and symmetry coordinates. The geometrical parameters of the molecule were allowed to relax and all the calculations converged to an optimized geometry which corresponds to a true minimum, as revealed by the lack of imaginary values in the wavenumber calculations. The Cartesian representation of the theoretical force constants have been computed at the fully optimized geometry by assuming C_s point group symmetry. The symmetry of the molecule was also helpful in making vibrational assignment. The transformation of force field, subsequent normal coordinate analysis and calculation of the PED were done on a PC with the MOLVIB program (version V7.0-G77) written by Tom Sundius [10].

Vibrational assignment

The molecule under consideration would belong to C_s point group and the 36 normal mode of fundamental vibrations, which span the irreducible representation 25A′+11A″. The A′ modes be polarized while the A″ modes be depolarized in the Raman spectrum. The harmonic vibrational modes calculated for 25DCA along with reduced mass, force constants Infrared intensities and Raman scattering activities have been summarized in Table 5. The FT-IR and FT-Raman spectra of 25DCA are shown in Fig 2 and Fig 3, respectively.

Root mean square (RMS) values of frequencies were obtained in the study using the following expression,

$$\text{RMS} = \sqrt{\frac{1}{n-1}\sum_{i}^{n}\left(\upsilon_i^{calc} - \upsilon_i^{exp}\right)^2}$$

The RMS error of the observed and calculated frequencies (unscaled / B3LYP/6-311+G**) of 25DCA was found to be 97 cm^{-1}. This is quite obvious; since the frequencies calculated on the basis of quantum mechanical force fields usually differ appreciably from observed frequencies. This is partly due to the neglect of a harmonicity and partly due to the approximate nature of the quantum mechanical methods. In order to reduce the overall deviation between the un scaled and observed fundamental frequencies, scale factors were applied in the normal coordinate analysis and the subsequent least square fit refinement algorithm resulted into a very close agreement between the observed fundamentals and the scaled frequencies. Refinement of the scaling factors applied in this study achieved a weighted mean deviation of 7.48 cm^{-1} between the experimental and scaled frequencies of the title compound.

Table 2. Optimized geometrical parameters of 25DCA obtained by B3LYP/6–311+G** density functional calculations

Bond length	Value(Å)	Bond angle	Value(Å)	Dihedral angle	Value(Å)
C2-C1	1.44599	C3-C2-C1	120.00020	C4-C3-C2-C1	-179.42806
C3-C2	1.38600	C4-C3-C2	120.00023	C5-C4-C3-C2	0.00000
C4-C3	1.38599	C5-C4-C3	119.99953	C6-C5-C4-C3	0.00000
C5-C4	1.38599	C6-C5-C4	120.00023	C7-C6-C5-C4	0.00000
C6-C5	1.38600	C7-C6-C5	120.00023	Cl8-C6-C5-C4	-179.42488
C7-C6	1.38599	Cl8-C6-C5	119.99882	Cl9-C3-C2-C1	1.14705
Cl8-C6	1.76006	Cl9-C3-C2	119.99882	H10-C1-C2-C7	-59.42979
Cl9-C3	1.76006	H10-C1-C2	120.00160	H11-C1-C2-C7	121.14686
H10-C1	1.02802	H11-C1-C2	119.99872	H12-C4-C3-C2	-179.42805
H11-C1	1.02805	H12-C4-C3	119.99899	H13-C5-C4-C3	-179.42805
H12-C4	1.12204	H13-C5-C4	119.99903	H14-C7-C6-C5	-179.42805
H13-C5	1.12205	H14-C7-C6	119.99899		
H14-C7	1.12204				

*for numbering of atom refer Fig 1

Table 3. Definition of internal coordinates of 25DCA

No(i)	symbol	Type	Definition
Stretching 1-6	r_i	C-C	C1-C2,C2-C3,C3-C4,C4-C5,C5-C6,C6-C1
7-9	S_i	C-H	C1-H8,C3-H10,C4-H11
10	p_i	C-N	C6-N7
11-12	P_i	C-Cl	C2-Cl9,C5-Cl12
13-14	n_i	N-H	N7-H13,N7-H14
Bending 15-20	α_i	C-C-C	C1-C2-C3,C2-C3-C4,C3-C4-C5, C4-C5-C6,C5-C6-C1,C6-C1-C2
21-26	θ_i	C-C-H	C6-C1-H8,C2-C1-H8,C2-C3-H10, C4-C3-H10,C3-C4-H11, C5-C4-H11
27-28	β_i	C-C-N	C1-C6-N7, C5-C6-N7
29-30	Φ_i	C-N-H	C6-N7-H13, C6-N7-H14
31	μ_i	H-N-H	H13-N7-H14
32-35	v_i	C-C-Cl	C1-C2-Cl9, C3-C2-Cl9, C4-C5-Cl12, C6-C5-Cl12
Out-of-plane 36-38	ω_i	C-H	H8-C1-C2-C6,H10-C3-C2-C4, H11-C4-C3-C5
39	ξ_i	C-N-H	C6-N7-H13-H14
40	Ω_i	C-N	N7-C6-C1-C5
41-42	ε_i	C-Cl	Cl9-C2-C3-C1,Cl12-C5-C6-C4
Torsion 43-48	τ_i	C-C	C1-C2-C3-C4,C2-C3-C4-C5, C3-C4-C5-C6,C4-C5-C6-C1, C5-C6-C1-C2,C6-C1-C2,C3
49	τ_i	N-H	C1(C5)-C6-N7-H13(H14)

*for numbering of atom refer Fig 1

Table 4. Definition of local symmetry coordinates and the value corresponding scale factors used to correct the force fields for 25DCA

No.(i)	Symbol[a]	Definition[b]	Scale factors used in calculation
1-6	C-C	r1,r2,r3,r4,r5,r6	0.914
7-9	C-H	S7,S8,S9	0.914
10	C-N	p10	0.992
11-12	C-Cl	P11,P12	0.992
13-14	N-H	n13, n14	0.995
15	C-C-C	$(\alpha15-\alpha16+\alpha17-\alpha18+\alpha19-\alpha20)/ \sqrt6$	0.992
16	C-C-C	$(2\alpha15-\alpha16-\alpha17+2\alpha18-\alpha19-\alpha20)/ \sqrt{12}$	0.992
17	C-C-C	$(\alpha16-\alpha17+\alpha19-\alpha20)/2$	0.992
18-20	C-C-H	$(\theta21-\theta22)/\sqrt2,(\theta23-\theta24)/\sqrt2, (\theta25-\theta26)/\sqrt2$	0.916
21	C-C-N	$(\beta27-\beta28)/\sqrt2$	0.923
22	C-N-H	$(\Phi29- \Phi30)/\sqrt2$	0.923
23	H-N-H	$\mu31$	0.990
24-25	C-C-Cl	$(v32- v33)/\sqrt2, (v34- v35)/\sqrt2,$	0.990
26-28	C-H	$\omega36, \omega37, \omega38$	0.994
29	C-N-H	$\xi39$	0.962
30	C-N	$\Omega40$	0.962
31-32	C-Cl	$\varepsilon41, \varepsilon42$	0.962
33	tring	$(\tau43-\tau44+\tau45-\tau46+\tau47-\tau48)/\sqrt6$	0.994
34	tring	$(\tau43-\tau45+\tau46-\tau48)/2$	0.994
35	tring	$(-\tau43+2\tau44-\tau45-\tau46+2\tau47-\tau48)/\sqrt{12}$	0.994
36	N-H	$\tau49/2$	0.979

[a] These symbols are used for description of the normal modes by TED in Table 5.
[b] The internal coordinates used here are defined in Table 3.

Table 5. Detailed assignments of fundamental vibrations of 25DCA by normal mode analysis based on SQM force field calculation

S. No.	Symmetry species C_s	Observed frequency (cm^{-1})		Calculated frequency (cm^{-1}) with B3LYP/6-311+G** force field				TED (%) among type of internal coordinates[c]
		Infrared	Raman	Unscaled	Scaled	IR[a] A_i	Raman[b] I_i	
1	A'	3675		3678	3674	22.431	49.945	NH(100)
2	A'		3574	3575	3571	32.823	148.594	NH(100)
3	A'			3545	3242	0.895	122.568	CH(99)
4	A'	3227		3225	3221	1.304	72.927	CH(99)
5	A'		3217	3215	3213	3.235	63.521	CH(99)
6	A'	1697		1695	1692	193.544	23.514	bHNH(59),CC(20),CN(13)
7	A'		1657	1658	1655	19.544	14.647	CC(57),bHNH(21),bCH(10),bring(8)
8	A'	1632		1631	1628	12.213	10.007	CC(69),bCH(11),bring(10)
9	A'			1550	1547	104.932	2.069	bCH(43),CC(40),CN(9)
10	A'	1483		1479	1476	26.645	0.543	CC(46),bCH(18),CN(16),bCCl(6),bCNH(5)
11	A'		1374	1375	1371	11.889	4.709	CC(81),bCH(7),bCNH(5)
12	A'	1336		1334	1331	18.643	5.150	bCH(46),CC(23),CN(19)
13	A'		1318	1316	1314	4.109	2.382	bCH(49),CC(30),CN(8),bCNH(5)
14	A'			1186	1183	7.415	2.583	bCH(62),CC(26),bCNH(8)
15	A'	1144		1142	1138	3.588	11.653	CC(42),bCH(27),bCNH(16),CCl(11)
16	A'		1116	1115	1113	91.628	0.329	bCNH(32),CC(32),CCl(17),bCH(9),bring(9)
17	A'	1063		1062	1059	37.583	13.607	bring(38),CC(30),CCl(19),bCNH(6)
18	A'		947	945	942	0.753	0.986	bCH(88),tring(11)
19	A'	927		932	928	44.088	0.636	bring(45),CCl(25),CN(12),CC(11)
20	A"		858	860	856	28.308	2.032	gCH(69),tring(19),gCN(7)
21	A"	805		806	803	24.038	1.974	gCH(85),tring(7),gCCl(6)
22	A'			726	724	0.778	18.460	bring(50),CCl(22),CC(22)
23	A"	713	710	712	709	6.074	0.657	tring(55),gCN(23),gCCl(16)
24	A"			610	608	43.369	0.453	tring(43),gCCl(28),gCN(12),gCNH(8)
25	A'	592		590	589	21.985	4.849	CCl(42),bring(40),CC(8)
26	A"		565	563	562	126.263	7.462	gCNH(36),bring(15),bHNH(12),bCN(8),CCl(7),bCCl(6)
27	A"			532	529	177.017	2.217	gCNH(48),bHNH(16),CN(12)
28	A'	456		455	453	6.192	1.301	bCN(34),bCCl(28),bring(13),CCl(11),CC(6)
29	A"		454	453	450	17.440	0.105	tring(60),gCCl(26),gCN(7),gCH(6)
30	A"			354	352	14.732	0.584	tNH2(74),gCCl(15),tring(5)
31	A'		333	336	332	0.064	9.270	bring(48),CCl(38),CC(9)
32	A"			304	301	7.943	1.390	gCCl(55),tring(18),tNH2(17),gCH(6)
33	A'		278	276	273	0.830	2.071	bCCl(52),bCN(31),bring(8)
34	A'			224	220	0.673	0.099	bCCl(89),CC(8)
35	A"		210	212	209	3.809	1.138	tring(66),gCH(15),gCCl(13)
36	A"			103	100	0.726	0.371	tring(67),gCCl(17),gCH(14)

Abbreviations used: b, bending; g, wagging; t, torsion; s, strong; vs, very strong; w, weak; vw, very weak;

[a] Relative absorption intensities normalized with highest peak absorption

[b] Relative Raman intensities calculated by Eq 1 and normalized to 100.

[c] For the notations used see Table 4.

Table 6. Mullikan's atomic charges of 25DCA based on B3LYP/6-311+G method**

S.No	Atom No.	B3LYP/6-311+G**
1	C1	-0.166951
2	C2	-0.072202
3	C3	-0.135598
4	C4	-0.139065
5	C5	-0.115709
6	C6	0.334071
7	N7	-0.790253
8	H8	0.158212
9	Cl9	-0.022910
10	H10	0.145938
11	H11	0.150135
12	Cl12	-0.028986
13	H13	0.337126
14	H14	0.346191

Table 7. The dipole moment (μ) and first-order hyperpolarizibility (β) of 25DCA derived from DFT calculations

β_{xxx}	**76354**
β_{xxy}	27449
β_{xyy}	-110.52
β_{yyy}	-816
β_{zxx}	-854.76
β_{xyz}	-849.9
β_{zyy}	-17.667
β_{xzz}	453.68
β_{yzz}	4000.9
β_{zzz}	93.234
β_{total}	67.112
μ_x	2.3673000
μ_y	0.00012628
μ_z	0.11840247
μ	0.34431443

Dipole moment (μ) in Debye, hyperpolarizibility $\beta(-2\omega;\omega,\omega)$ 10^{-30}esu.

Table 8. Computed absorption wavelength (λ_{ng}) , energy (E_{ng}), oscillator strength (f_n) and its major contribution

n	λ_{ng}	E_{ng}	f_n	Major contribution
1	202.4	6.13	0.0193	H-0->L+0(+48%), H-1->L+1(27%)
2	198.3	6.25	0.0291	H-0->L+1(44%), H-1->L+0(30%)
3	171.6	7.23	0.0009	H-0->L+2(+69%)

(Assignment; H=HOMO,L=LUMO,L+1=LUMO+1,etc.)

C–H vibrations

Aromatic compounds commonly exhibit multiple weak bands in the region 3300–3100 cm^{-1} due to aromatic C–H stretching vibrations. Accordingly, in the present study the C–H vibrations of the title compounds are observed at 3227, 3225 and 3221 cm^{-1} in the FT-IR spectrum and 3217, 3215 and 3213 cm^{-1} in Raman for 25DCA. The bands due to C–H in-plane ring bending vibration interacting with C–C stretching vibration are observed as a number of m-w intensity sharp bands in the region 1300–1000 cm^{-1}. C–H out-of-plane bending vibrations are strongly coupled vibrations and occur in the region 900–667 cm^{-1}. The in-plane and out-of-plane bending vibrations of C–H have also been identified for the title compound.

Ring vibrations

The aromatic ring modes predominantly involve C–C bonds. The vibrational frequency 1756-1608 cm^{-1} corresponds to stretching and contraction of the other part of the ring [11]. The scaled frequencies of 454, 453 and 450 cm^{-1} show the out-of-plane bending modes of the ring carbons. The in-plane ring bending vibrations are observed at 592, 590 and 589 cm^{-1}. The other theoretically calculated C–C–C out-of-plane and in-plane

bending modes have been found to be consistent with the recorded spectral values. The ring breathing mode is assigned at 1063 cm^{-1} owing to its characteristic intensity and depolarization features in the IR spectrum. In the case of 25DCA the Raman frequency at 1116, 1115 and 1113 cm^{-1} assigned to ring breathing mode [12]. In the present case a very strong FT-IR band at 927 cm^{-1} and a weak FT-Raman band at 947 cm^{-1} are assigned to ring breathing mode.

C-C vibrations

The ring C–C stretching vibrations, usually occur in the region 1700–1495 cm^{-1}. Hence in the present investigation, the FT-IR bands indentified at 1697, 1695, 1692, 1632, 1631, 1628 cm^{-1} and the FT-Raman bands at 1658, 1657, 1655 cm^{-1} are assigned to C–C stretching vibrations of 25DCA. The band ascribed at 1144, 1142 and 1138 cm^{-1} in FT-IR and 1116, 1115 and 1113 cm^{-1} in FT-Raman spectra has been designated to C-C in-plane bending mode.

C-N vibrations

The IR and Raman bands observed between 1336, 1334, 1331 cm^{-1} and 1318, 1316, 1314 cm^{-1} in the title compounds have been assigned to C-N stretching vibrations. The in-plane

and out-of-plane bending vibrations assigned in this study are also supported by the literature [13]. For the title compounds a pure mode cannot be expected for this vibration since it falls in a complicated region of the vibrational spectrum.

C–Cl vibrations

The C–Cl stretching frequency is generally observed in the region 800–500 cm^{-1} depending on the configuration and conformation of the compound. In present investigation, the FT-IR and Raman bands observed at 806, 805, 803, 713, 592, 590, 589 cm^{-1} and 712, 710, 709 cm^{-1} has been assigned to C–Cl stretching modes show strong mixing with several planar modes. However, the C–Cl bending modes appear to be relatively pure modes. The C–Cl out of plane bending modes was identified at 456, 455, 453 cm^{-1} and 565, 563, 562, 454, 453, 450, 336, 333, 332, 278, 212 and 209 cm^{-1} for IR and Raman, respectively.

Amino group vibrations

According to Socrates [14] the stretching, scissoring and rocking deformation of amino group appeared around 4000–3000, 1700–1600 and 1150–900 cm^{-1}, respectively, in the absorption spectra. In 25DCA, the antisymmetric and symmetric stretching modes of NH$_2$ group found at 3678, 3675, 3674, 3575, 3574 and 3571 cm^{-1}, respectively. The scissoring, rocking, wagging and twisting modes of NH$_2$ group presented in 25DCA were identified well within their characteristic regions. These modes are observed at 1697, 1695, 1692, 1483, 1479, 1476 cm^{-1} and 1658, 1657, 1655 cm^{-1} in FT-IR and FT-Raman spectrum.

Mulliken population analysis

The values of the Mullikan's atomic charges on each atom of the title compound were also obtained with the help of B3LYP level of the theory incorporating 6-311+G** basis set. The total atomic charges on each atom of the title compound are presented in Table 5.6.

First-order hyperpolarizability calculations

The first-order hyperpolarizabilities (β_0) of this novel molecular system, and related properties β_0, α_0 and $\Delta\alpha$) of 25DCA were calculated using B3LYP/6-311+G** basis set, based on the finite-field approach. In the presence of an applied electric field, the energy of a system is a function of the electric field. Polarizabilities and hyperpolarizabilities characterize the response of a system in an applied electric field [15]. They determine not only the strength of molecular interactions (long-range inter induction, dispersion force, etc.) as well as the cross sections of different scattering and collision process but also the nonlinear optical properties (NLO) of the system [16,17]. First-order hyperpolarizability is a third rank tensor that can be described by $3 \times 3 \times 3$ matrix. The 27 components of the 3D matrix can be reduced to 10 components due to the Kleinman symmetry [18]. It can be given in the lower tetrahedral format. It is obvious that the lower part of the $3 \times 3 \times 3$ matrixes is a tetrahedral. The components of β are defined as the coefficients in the Taylor series expansion of the energy in the external electric field. When the external electric field is weak and homogeneous, this expansion becomes:

$$E = E^0 - \mu_\alpha F - 1/2\alpha_{\alpha\beta}F_\alpha F_\beta - 1/6\beta_{\alpha\beta\gamma}F_\alpha F_\beta F_\gamma + ...$$

The total static dipole moment is

$$\mu = (\mu_x^2 + \mu_y^2 + \mu_z^2)^{1/2}$$

and the average hyperpolarizability is

$$\beta_0 = (\beta_x^2 + \beta_y^2 + \beta_z^2)^{1/2}$$

and

$$\beta_x = \beta_x + \beta_{xyy} + \beta_{xzz}$$

$$\beta_y = \beta_{yyy} + \beta_{xyy} + \beta_{xzz}$$

$$\beta_x = \beta_x + \beta_{xyy} + \beta_{xzz}$$

The B3LYP/6-311+G** calculated first-order hyperpolarizability of 25DCA is 67.112x10^{-30} esu is shown in Table 7. Electronic excitation energies, oscillator strength and nature of the respective excited states were calculated by the closed-shell singlet calculation method and are summarized in Table 8. Fig 4 shows the highest occupied molecule orbital (HOMO) and lowest unoccupied molecule orbital (LUMO) of 25DCA. Orbital involved in the electronic transition for (a) HOMO−0 (b) LUMO+0 (c) HOMO-1 (d) LUMO+1 (e) LUMO+2 is represented in Fig. 5.5. The NLO responses can be understood by examining the energetic of frontier molecular orbitals. There is an inverse relationship between hyperpolarizability and HOMO–LUMO.

HOMO energy = -0.002 a.u
LUMO energy = 0.016 a.u
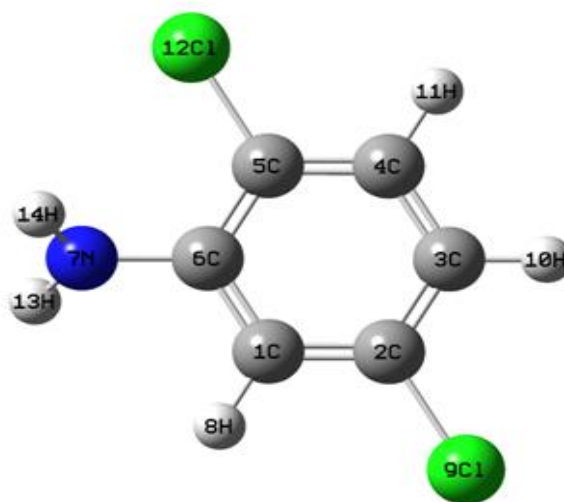HOMO–LUMO energy gap = 0.018 a.u

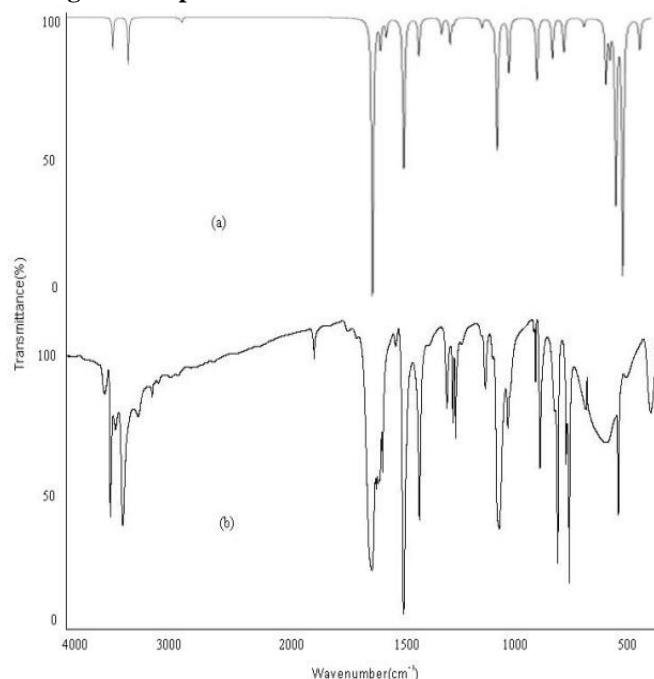**Fig 1. The optimized molecular structure of 25DCA**

Fig 2. FT-IR spectra of 25DCA
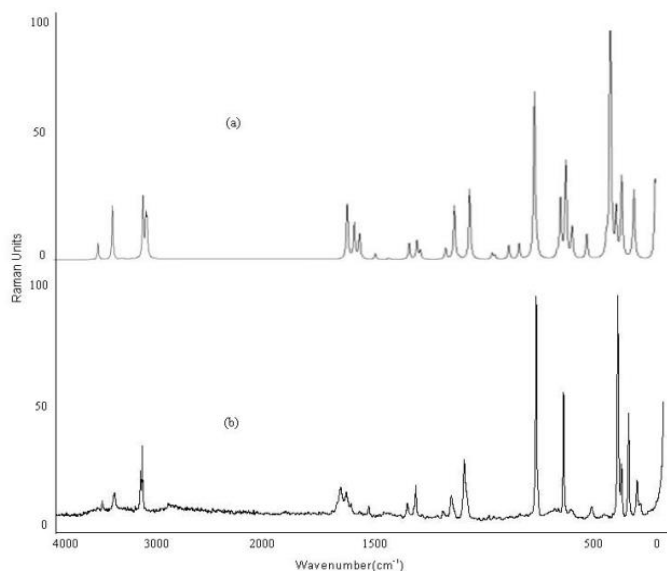**(a)Calculated (b) Observed with B3LYP/6-311+G****

Fig 3. FT-Raman spectra of 25DCA
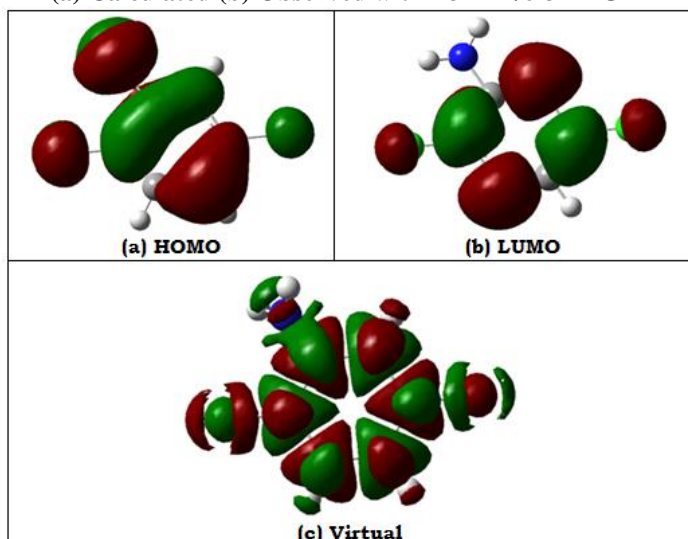**(a) Calculated (b) Observed with B3LYP/6-311+G****

Fig 4. Representation of the orbital involved in the electronic transition for (a) HOMO (b) LUMO (c) Virtual
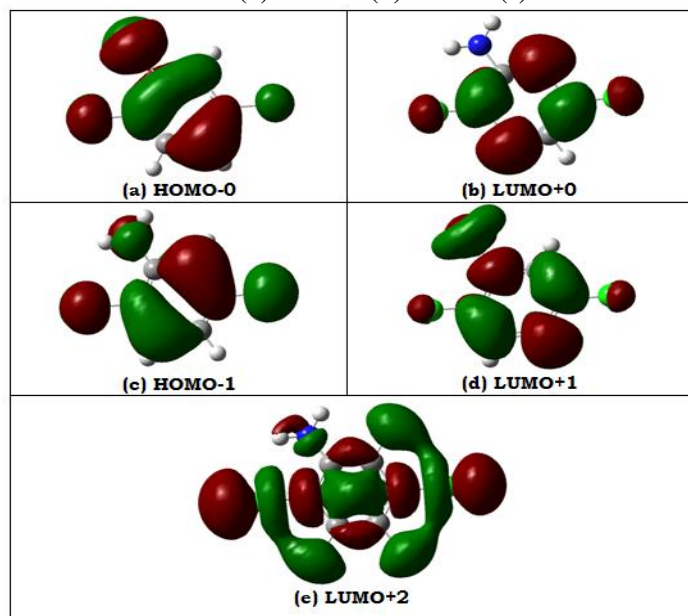

Fig 5. Representation of the orbital involved in the electronic transition for (a) HOMO−0 (b) LUMO+0 (c) HOMO-1 (d) LUMO+1 (e) LUMO+2

Conclusions

Attempts have been made in the present work for the proper frequency assignments for the compound 25DCA. The FT-IR and FT-Raman spectra were recorded. The equilibrium geometries and harmonic frequencies of 25DCA were determined and analysed at DFT level of theories utilizing B3LYP/6-311+G** basis sets. The difference between the observed and scaled wave number values of most of the fundamentals is very small. Any discrepancy noted between the observed and the calculated frequencies may be due to the fact that the calculations have been actually done on single molecules in the gaseous state contrary to the experimental values recorded in the presence of intermolecular interactions. The values of the Mullikan's atomic charges on each atom of the title compound were also obtained. The first-order hyperpolarizability (β_{total}) of 25DCA was calculated and found to be 67.112×10^{-30} esu. Electronic excitation energies, oscillator strength and nature of the respective excited states were calculated by the closed-shell singlet calculation method. The NLO responses can be understood by examining the energetic of frontier molecular orbitals.

References

1. M. J. Frisch, G. W. Trucks, H. B. Schlegel, G. E. Scuseria, M. A. Robb, J. R. Cheeseman, G. Scalmani, V. Barone, B. Mennucci, G. A. Petersson, H. Nakatsuji, M. Caricato, X. Li, H. P. Hratchian, A. F. Izmaylov, J. Bloino, G. Zheng, J. L. Sonnenberg, M. Hada, M. Ehara, K. Toyota, R. Fukuda, J. Hasegawa, M. Ishida, T. Nakajima, Y. Honda, O. Kitao, H. Nakai, T. Vreven, J. A. Montgomery, Jr., J. E. Peralta, F. Ogliaro, M. Bearpark, J. J. Heyd, E. Brothers, K. N. Kudin, V. N. Staroverov, R. Kobayashi, J. Normand, K. Raghavachari, A. Rendell, J. C. Burant, S. S. Iyengar, J. Tomasi, M. Cossi, N. Rega, J. M. Millam, M. Klene, J. E. Knox, J. B. Cross, V. Bakken, C. Adamo, J. Jaramillo, R. Gomperts, R. E. Stratmann, O. Yazyev, A. J. Austin, R. Cammi, C. Pomelli, J. W. Ochterski, R. L. Martin, K. Morokuma, V. G. Zakrzewski, G. A. Voth, P. Salvador, J. J. Dannenberg, S. Dapprich, A. D. Daniels, O. Farkas, J. B. Foresman, J. V. Ortiz, J. Cioslowski, and D. J. Fox, Gaussian, Inc., Wallingford CT, 2009.
2. A.D. Becke, J. Chem. Phys., 98 (1993) 5648.
3. C. Lee, W. Yang, R.G. Parr, Phys. Rev., B37 (1988) 785.
4. P. Pulay, G. Fogarasi, G. Pongor, J.E. Boggs, A. Vargha, J.Am. Chem. Soc., 105 (1983) 7037.
5. M.A. Pasha, Aisha Siddekha, Soni Mishra, Sadeq Hamood Saleh Azzam, S. Umapathy, Spectrochimica Acta Part A: Molecular and Biomolecular Spectroscopy, In Press, Accepted Manuscript, Available online 5 October 2014.
6. G. Socrates, Infrared and Raman Characteristic Group Frequencies – Tables and Charts, third ed., J. Wiley & Sons, Chichester, 2001.
7. B. Wojtkowaik, M. Chabanel, Spectrochimie Moleculaire Technique et Documentation, Paris, 1977.
8. P.L. Polavarapu, J. Phys. Chem. 94 (1990) 8106.
9. G. Keresztury, S. Holly, J. Varga, G. Besenyei, A.Y. Wang, J.R. Durig, Spectrochim. Acta 49A (1993) 2007.
10. T. Sundius, J. Mol. Struct., 218 (1990) 321.
11. R. Zwarich, J. Smolarck, L. Goodman, J. Mol. Spectrosc. 38 (1971) 336.(2012) 728-736.
12. Hacer Pir Gümüş, Ömer Tamer, Davut Avcı, Yusuf Atalay, Spectrochimica Acta Part A: Molecular and Biomolecular Spectroscopy, 132 (2014) 183-190.
13. M. Arivazhagan, S. Manivel, S. Jeyavijayan and R. Meenakshi, Spectrochimica Acta Part A: Molecular and Biomolecular Spectroscopy, 134 (2015) 493-501.

14. G. Socrates, Infrared and Raman Characteristic Group Frequencies – Tables and Charts, third ed., J. Wiley & Sons, Chichester, 2001.

15. C.R. Zhang, H.S. Chen, G.H. Wang, Chem. Res. Chin. U. 20 (2004) 640–646.

16. Y. Sun, X. Chen, L. Sun, X. Guo, W. Lu, J. Chem. Phys. Lett. 381 (2003) 397–403.

17. O. Christiansen, J. Gauss, J.F. Stanton, J. Chem. Phys. Lett. 305 (1999) 147–155.

18. D.A. Kleinman, Phys. Rev. 1962;126,1977.